ASME 2012 5th Annual Dynamic Systems and Control Conference joint with the JSME 2012 11th Motion and Vibration Conference
DSCC2012-MOVIC2012
October 17-19, 2012, Fort Lauderdale, Florida, USA

DSCC2012-MOVIC2012-8781

MECHANICS AND CONTROL OF QUADROTORS FOR TOOL OPERATION

Dongjun Lee* **and Changsu Ha**
School of Mechanical & Aerospace Engineering and Institute of Advanced Machinery & Design
Seoul National University, Seoul, Korea, 151-744.
Email: {djlee, changsuha}@snu.ac.kr.

ABSTRACT

We consider the following two problems to enable a quadrotor to operate a mechanical tool (e.g., screwdriver, vertical jack, etc), which is rigidly-attached on the quadrotor and whose control, different to other quadrotor motion control results, demands an *integrated and simultaneous* control of the quadrotor's translation and rotation: 1) tool-tip position trajectory tracking control; and 2) tool rotating operation control with the tool-tip position regulated. We characterize some structural conditions for generating any arbitrary desired control for the tool-tip position and also for avoiding internal dynamics instability (with possible finite-time escape). Simulations are performed to support the theory.

1 Introduction

As pointed out in [1], by extending the 2-dimensional mobility of usual (wheeled) mobile robots to the 3-dimensional space, unmanned aerial vehicles are promising to realize many powerful applications, both outdoor and indoor: landscape survey, remote camera work for movie/commercial making, surveillance and reconnaissance, remote repair of infrastructure, operation on high-rise building exterior, manufacturing and logistics automation, and even human-assistive household flying agents, to name just few. See also [2].

Among the unmanned aerial vehicles, due to the affordability and relative easiness to control, the quadrotors have recently been studied extensively and numerous strong control results have been proposed for them (e.g., motion control [3–7], acrobatic flying [8, 9], teleoperation [10, 11], distributed coordination [12–14], cooperative transport [15, 16]). However, the problem of how to utilize the quadrotors for mechanical manipulation tasks (e.g., force-controlled assembly; surface deburring; tool operation) has been largely unexplored, although this manipulation capability would make the quadrotors a truly versatile and powerful robotic platform.

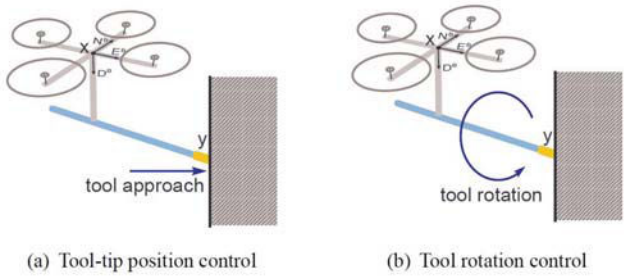

(a) Tool-tip position control (b) Tool rotation control

Figure 1. Quadrotor tool operation control modes

This paper is concerned with this quadrotor mechanical manipulation problem. More specifically, we consider the cases, where a quadrotor has a mechanical tool (e.g., screwdriver, wrench, vertical jack, etc) rigidly attached on it and is required to operate (or often rotate) the tool by simultaneously controlling its position and orientation. For this quadrotor tool operation, we particularly consider the following two, perhaps most essential, behaviors for the tool operation and propose novel control frameworks to achieve them: 1) tool-tip position tracking control (Fig. 1-(a)); and 2) tool rotating control with the tool-tip position fixed (Fig. 1-(b)).

For this, we first rewrite the quadrotor's translation dynamics w.r.t. the tool-tip position $y \in \Re^3$ while assuming that the tool addition is light enough as compared to the quadrotor itself. We then show that any desired control action $u \in \Re^3$ can be generated, if and only if the tool-tip position y is not contained within the (N^B, E^B)-plane (see Fig. 2). We then elucidate the internal dynamics [17], which is "hidden" from this desired control u generation, and show that, if the tool-tip position y is below

*Address all correspondence to this author.

(i.e., downward) the (N^B, E^B)-plane, this internal dynamics will become unstable even with a possibility of finite-time escape, suggesting to set the tool-tip position y to be (perhaps counter-intuitively) above (i.e., upward) the center-of-mass position x to avoid internal instability. Based on these observations, we then derive novel control frameworks for: 1) trajectory tracking control of the tool-tip position y; and 2) tool rotation control while keeping the tool-tip position y regulated.

To our knowledge, these two control problems cannot be addressed by most (if not all) of other available quadrotor control results (e.g. [3–7]), since those results are usually only concerned with the motion control of the center-of-mass x-position, whereas these two problems require an *integrated* control of the quadrotor's rotation and the center-of-mass x-position at the same time (e.g., note that y depends both on x and the quadrotor's orientation matrix $R \in \Re^{3\times 3}$).

The rest of this paper is organized as follows. The standard system modeling of the quadrotor is reviewed in Sec. 2. The dynamics of the tool-tip position y is then given in Sec. 3, along with the structural requirement for the desired control u-generation and the discussion on the internal dynamics stability. Trajectory tracking control for the y-position and the tool-rotating control (y-fixed) are then proposed in Sec. 4 with relevant simulation results, and some concluding remarks are given in Sec. 5.

2 Quadrotor Modeling

Let us consider a quadrotor as shown in Fig. 2, which is evolving in SE(3) with the following dynamics:

$$m\ddot{x} = -\lambda R e_3 + mge_3 + f_e \tag{1}$$
$$J\dot{w} + w \times Jw = \tau + \tau_c, \quad \dot{R} = RS(w) \tag{2}$$

where $x \in \Re^3$ is the quadrotor's center-of-mass position represented in the inertial frame $\{O\} := \{N^o, E^o, D^o\}$, $m > 0$ is the mass, $\lambda \in \Re$ is the thrust, $R \in SO(3)$ represents the rotation of the body-frame $\{B\} := \{N^B, E^B, D^B\}$ w.r.t. the inertial-frame $\{O\}$, $f_e \in \Re^3$ is the tool force represented in $\{O\}$, g is the gravitation constant, and $e_3 = [0,0,1]^T$ is the basis vector specifying the down direction. Also, $J \in \Re^{3\times 3}$ is the body-frame rotational inertia, $w_i := [w_1; w_2; w_3]^T \in \Re^3$ is the angular velocity of $\{B\}$ relative to $\{O\}$ represented in $\{B\}$, $\tau, \tau_c \in \Re^3$ are the torque input and tool torque, all represented in $\{B\}$ frame, and

$$S(w) = \begin{bmatrix} 0 & -w_3 & w_2 \\ w_3 & 0 & -w_1 \\ -w_2 & w_1 & 0 \end{bmatrix} \quad \text{s.t.} \quad S(w)v = w \times v \tag{3}$$

for any $v \in \Re^3$.

This dynamics (1)-(2) is has been widely used for the quadrotor's center-of-mass position *motion control* [3–6, 13].

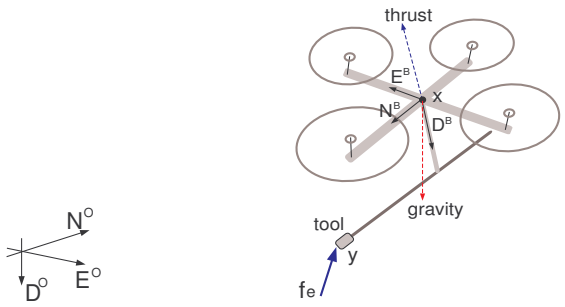

Figure 2. Quadrotor with a tool: $\{O\} := \{N^o, E^o, D^o\}$ and $\{B\} := \{N^B, E^B, D^B\}$ are the inertial and body frames, with thrust and gravity along D^B and D^o; tool attached at $d = [d_1, 0, d_3] \in \Re^3$ in $\{B\}$.

Different to those results, in this paper, we consider the control problem for mechanical tool operation (e.g., screwdriver, wrench, etc), which is rigidly-attached to the quadrotor at the point $d = [d_1; 0; d_3] \in \Re^3$ from x as measured in $\{B\}$. See Fig. 2. For this, we assume that the tool addition is light enough (with also some suitable counter-balancing) so that x in (1) can still adequately specify the total system's center-of-mass position. We also assume that the tool interacts with the environment through the Cartesian force f_e and the reaction moment τ_e so that

$$\tau_c = d \times R^T f_e + R^T \tau_e \tag{4}$$

where d is the distance between y and x represented in the $\{B\}$ frame, and $R^T f_e$ and $R^T \tau_e$ are the interaction force f_e and torque τ_e also represented in the $\{B\}$ frame.

3 Dynamics of Tool-Tip Position y

Different to many other quadrotor's x-position control results [3–6, 13], for the tool operation, we would like to directly drive the tool-tip position y (e.g., tool approaching behavior) or to regular this y while rotating the quadrotor (e.g., for operating wrench or screwdriver). For this, here, we convert the x-dynamics (1) to the y-dynamics. First, note that we have

$$y = x + Rd, \quad \dot{y} = \dot{x} + \dot{R}d = \dot{x} + RS(w)d$$
$$\ddot{y} = \ddot{x} + R[S(\dot{w}) + RS^2(w)]d$$

using (2), where

$$S^2(w) = \begin{bmatrix} -w_2^2 - w_3^2 & w_1 w_2 & w_3 w_1 \\ w_1 w_2 & -w_3^2 - w_1^2 & w_2 w_3 \\ w_3 w_1 & w_2 w_3 & -w_1^2 - w_2^2 \end{bmatrix}. \tag{5}$$

Then, we can rewrite (1) s.t.

$$m\ddot{y} - mR[S(\dot{w}) + S^2(w)]d = -\lambda R e_3 + mge_3 + f_e \tag{6}$$

which describes the dynamics of the y-point.

3.1 Structural Requirement for y-Control

In (6), we may consider λ and $\dot{w}$ as the control inputs, since we can directly affect $\dot{w}$ by τ through (2). Now, suppose that we want to drive (or regulate) the y-point via a certain desired control u (e.g., $u = -b\dot{y} - ky$). This then can be achieved if we can control λ, τ s.t., for (6),

$$mR[S(\dot{w}) + S^2(w)]d - \lambda Re_3 + mge_3 = u \tag{7}$$

which can also be rewritten as

$$m \begin{bmatrix} 0 & -d_3 & d_2 \\ d_3 & 0 & -d_1 \\ -d_2 & d_1 & 0 \end{bmatrix} \begin{pmatrix} \dot{w}_1 \\ \dot{w}_2 \\ \dot{w}_3 \end{pmatrix} + \begin{pmatrix} 0 \\ 0 \\ \lambda \end{pmatrix} = R^T[-u + mge_3 + mRS^2(w)d] \tag{8}$$

where $d_2 = 0$ and we use $S(\dot{w})d = -S(d)\dot{w}$. From this, we can see that we have four control inputs available $(\lambda, \dot{w})$ to directly affect the y-dynamics. That is, for the y-dynamics, we do not have the under-actuation issue of the x-dynamics (1) (i.e., $x \in \Re^3$ with only one control $\lambda \in \Re$), to address which some (indirect) means should be deployed in the control design (e.g., backstepping [4, 13]). Note also that, here, we may also include the f_e-information in the desired control u, if the force sensing of f_e is available.

Proposition 1 *Given* $(\lambda, \dot{w}_1, \dot{w}_2, \dot{w}_3)$ *as the control input, the LHS of* (8) *can produce any vector in* $\Re^3$ *if and only if* $d_3 \neq 0$.

Proof: If $d_3 \neq 0$, we can produce any values for the first and second rows in the LHS of (8) by $\dot{w}_1, \dot{w}_2$, while for the last row by λ. On the other hand, if $d_3 = 0$, the first and second rows are generated only by the one value $\dot{w}_3$, thus, cannot assume arbitrary values. ■

This Prop. 1 implies that, to achieve a desired control u directly for the y-dynamics, we must have $d_3 \neq 0$, i.e., there should be a non-zero downward offset (i.e., along D^B) between x and y. As long as $d_3 \neq 0$, we would then be able to reproduce any desired $u \in \Re^3$ by recruiting λ and τ (i.e. $\dot{w}$). This Prop. 1 also implies that: 1) we would not be able to control the tool-tip position $y \in \Re^3$ arbitrarily if we attach the tool at the center-of-mass x and parallel to the quadrotor's body (i.e., $d_3 = 0$ with $d_1 \neq 0$); and 2) for dexterous operation of the tool position y, we should set some upward or downward offset d_3 when attaching the tool.

3.2 Internal Dynamics

Suppose that we control λ, τ to generate the desired control u from (7) (with $d_3 \neq 0$). Then, we will have

$$m\ddot{y} = u + f_e$$

that is, it may now appear that we can indeed control the y-dynamics however as specified by the desired control u. Yet, for this control u to be really achievable, the internal dynamics [17], "hidden" from the above y-dynamics, should be stable (or stabilizable). That is, from (7), we have

$$m[S(\dot{w}) + S^2(w)]d - \lambda e_3 + mgR^T e_3 = R^T u =: u' \tag{9}$$

which defines the internal dynamics of $\dot{w}, w, R$ given u'.

Now, suppose that a certain tool operation requires the quadrotor to rotate about the N^o-axis with $N^B = N^o$ (e.g., screwdriver operation about N^o-axis, etc). For this case, the quadrotor's rotation matrix R can be written as

$$R = \begin{bmatrix} 1 & 0 & 0 \\ 0 & \cos\theta & -\sin\theta \\ 0 & \sin\theta & \cos\theta \end{bmatrix} \tag{10}$$

where $\dot{\theta} = w_1$ and $w = [w_1; 0; 0]$. Then, using (3) and (5), we can rewrite the internal dynamics (9) w.r.t. the $\{B\}$-frame s.t.

$$\begin{pmatrix} 0 \\ -md_3\dot{w}_1 + mg\sin\theta \\ -md_3w_1^2 - \lambda + mg\cos\theta \end{pmatrix} = u' \tag{11}$$

where the dynamics in the second row is similar to the pendulum dynamics, which will be unstable if $d_3 > 0$ (i.e., downward offset of the tool-tip y from x). If this internal dynamics is stabilized, we may then assign (bounded) λ in the third-row to realize the desired control u; if not, we would not be able to really apply the desired control u. That is, we need $d_3 < 0$ (i.e., upward offset of the tool-tip y from x) to avoid unstable internal dynamics. Note also that, in (11), we should have $u'_1 = 0$, since, here, we assume no rotation of the quadrotor about E^B-axis or D^B-axis and the thrust λ is along D^B-axis.

On the other hand, consider the case where the tool operation requires the quadrotor to rotate about the E^o-axis with $E^B = E^o$ (e.g., vertical jack operation, etc). For this case, we may write R s.t.

$$R = \begin{bmatrix} \cos\theta & 0 & \sin\theta \\ 0 & 1 & 0 \\ -\sin\theta & 0 & \cos\theta \end{bmatrix} \tag{12}$$

with $w = [0; w_2; 0]$ and $\dot{\theta} = w_2$. Then, similar to (11), we can obtain the following internal dynamics in the $\{B\}$-frame:

$$\begin{pmatrix} md_3\dot{w}_2 - md_1w_2^2 - mg\sin\theta \\ 0 \\ -md_1\dot{w}_2 - md_3w_2^2 - \lambda + mg\cos\theta \end{pmatrix} = u' \tag{13}$$

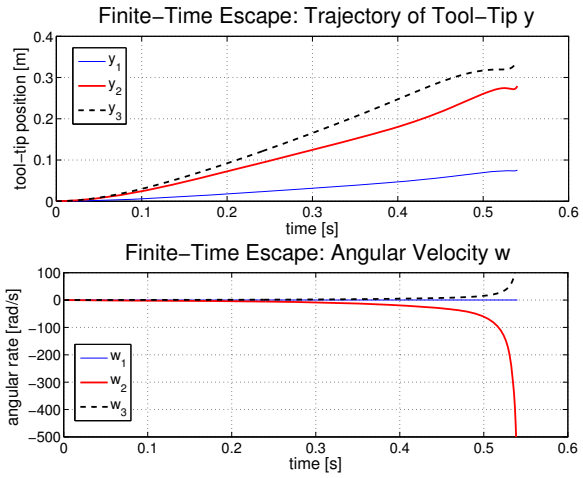

Figure 3. Finite-time escape with $d_3 = 0.2$[m]: 1) trajectory of tool-tip position y; and 2) angular rate w.

where the condition $d_3 > 0$ is even more problematic, since, with $d_3 > 0$, the dynamics in the first row of (13) would not only be unstable but also contain, if $d_1 \neq 0$, the quadratically-growing term $md_1w_2^2$, which can trigger a finite-time escape [17]. See Fig. 3. Note that, however, if $d_3 < 0$, this dynamics, even with the quadratic term $md_1w_2^2$, will be locally exponentially stable.

Although our observation so far on the stability of internal dynamics (9) is limited to the specific rotational motions of the quadrotor, given the high likelihood of occurrence of these two rotational motions during general tool operations, we believe the suggested condition $d_3 < 0$ would be relevant to many quadrotor tool operation scenarios, as captured by the following Prop. 2.

Proposition 2 *Given an arbitrary desired control $u(t)$, the internal dynamics* (9) *is stable only if $d_3 < 0$.*

This Prop. 2 may look un-intuitive at the first glance, as the tool attached below the quadrotor (i.e., $d_3 > 0$) would likely sound more favorable to the system's stability. However, as depicted in Fig. 4, since the gravity pulls not the y-position but the x-position, this gravity will produce a *positive-feedback* for the rotational θ-motion if $d_3 > 0$ similar to the case of inverted pendulum; or a *negative-feedback* if $d_3 < 0$, similar to the case of stable downward pendulum. Note that, even if the tool-addition is not so light as compared to the quadrotor, the condition $d_3 < 0$ would still be relevant for the stability of internal dynamics (9), since, in this case, the center-of-mass position will still be above the y-position, thereby, produces a positive-feedback with $d_3 > 0$.

In the following two sections, we design two control laws for the quadrotor, one to drive the tool-tip position y to track a desired timed-trajectory and the other to rotate the tool rigidly-attached to the quadrotor with the tool-tip position y regulated, while addressing this issue of internal dynamics stability. Note that these two control objectives cannot be attained by using the

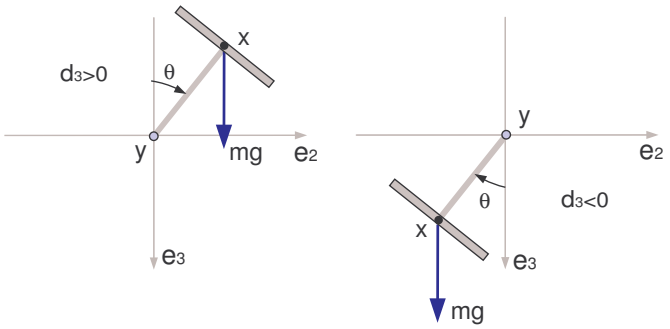

Figure 4. Effect of d_3 on internal dynamics: 1) if $d_3 > 0$, gravity serves as positive-feedback; 2) if $d_3 < 0$, as negative-feedback.

standard quadrotor control results (e.g., [3–6, 13]), since, in contrast to those, here, we need to control not only the quadrotor's center-of-mass position x but also its rotation R in an integrated way, as the tool-tip y-position (6) depends both on x and R.

4 Control Design for Quadrotor Tool Operation

4.1 Tool-Tip Position Tracking Control

One of the most basic behaviors for the quadrotor tool operation is to drive the tool-tip position y toward a certain work site location. See Fig. 1-(a). For this, in this section, we consider a trajectory tracking control for the y-position, that is, $(y, \dot{y}, \ddot{y}) \to (y_d, \dot{y}_d, \ddot{y}_d)$, where $y_d(t) \in \Re^3$ is a desired timed-trajectory for the y-position. We then design the desired control u in (7) s.t.

$$u := m\ddot{y}_d - b(\dot{y} - \dot{y}_d) - k(y - y_d) \tag{14}$$

with which the closed-loop y-dynamics becomes

$$m\ddot{e} + b\dot{e} + ke = f_e$$

where $e := y - y_d$, and $b, k > 0$ are the control gains. Here, since there is no mechanical interaction between the quadrotor and the environment, we have $f_e \approx 0$. Thus, we will have $(\dot{e}, e) \to 0$ exponentially.

To achieve this desired tracking control u (14), we define the desired angular acceleration $\dot{w}^d = [\dot{w}_1^d; \dot{w}_2^d; \dot{w}_3^d] \in \Re^3$ and the thrust control λ through (8), which can be rewritten as

$$\begin{pmatrix} -md_3\dot{w}_2^d \\ md_3\dot{w}_d^1 \\ md_1\dot{w}_2^d + \lambda \end{pmatrix} = R^T[-u + mge_3] + mRS^2(w)d =: \nu'$$

with $d_2 = 0$. From this, we can then compute $\dot{w}_1^d = \nu_2'/(md_3)$, $\dot{w}_2^d = -\nu_1'/(md_3)$ and $\lambda = \nu_3' - md_1\dot{w}_2^d = \nu_3' + (d_1/d_3)\nu_1'$.

To drive $\dot{w} \to \dot{w}^d$, we then design the attitude control torque τ for (2) s.t.

$$\tau = w \times Jw + J\left(\dot{w}^d - \alpha\left[w - \int_0^t \dot{w}^d(\tau)d\tau\right]\right) - \beta w \qquad (15)$$

where $\alpha, \beta > 0$ are the control gains. Then, since $\tau_c \approx 0$ (from $f_e, \tau_e \approx 0$), the closed-loop attitude dynamics is reduced to

$$J[\dot{e}_w + \alpha e_w] + \beta w = 0$$

where $e_w(t) := w(t) - \int_0^t \dot{w}^d(\tau)d\tau$, implying that, if $\beta w \approx 0$, $\dot{w} \to \dot{w}_d$. Here, we adopt the term βw for (15), although it may degrade the y-tracking performance, since we found that some small damping β turns out to be useful: 1) to reduce $||w(t)||$ during both the operation start and the steady-state (i.e., R motion); and 2) to mitigate the possibility of finite-time escape (by reducing the quadratic term in (13)). Moreover, in steady-state, we often observe $w \to 0$ (see Fig. 5).

Simulations are performed with this tool-tip trajectory tracking control. For this, we assume 3% parametric uncertainty in the mass/inertia estimates and also 5% error in the measurement of f_e (this $f_e = 0$ for the tracking simulation; whereas $f_e \neq 0$ for the tool rotating operation - see below). The results (with $d = (0.3, 0, -0.2)$[m]) are shown in Fig. 5, where we can see that: 1) the tool-tip position y can track a saddle-like desired trajectory $y_d \in \Re^3$; and 2) the control actions λ, τ and the angular rate w gradually converge to their steady-state values. Here, the tracking error and w both exhibit some low-frequency oscillation. This is because we assume some parametric uncertainty in computing the control action, through which the periodic desired trajectory acts as a sinusoid disturbance.

4.2 Tool Rotation Control

Here, we would like to rotate the quadrotor (i.e., also the attached tool) while keeping the tool-tip position y regulated. See Fig. 1-(b). From (6), we can then see that, if we incur any rotation motion, it will produce some force, that will perturb the y-dynamics, if not absorbed by the interaction force f_e. In other words, to keep the tool-tip position y fixed, we should have: from (6) with $\ddot{y} = 0$,

$$-f_e = mR[S(\dot{w}) + S^2(w)]d - \lambda R e_3 + mge_3 \qquad (16)$$

where $-f_e$ is the contact force between the tip-position y and the work site. Here, we consider the case where: 1) we need to regulate the magnitude of this f_e to be small; and 2) we can dominate τ_c in (2) by the control τ. A scenario, which is relevant to this assumption and also envisioned for future experimental implementation, is where the tool's d_1-axis (i.e., N^B-direction) slides into a keyed-hole and the tool-tip is locked at the end of the hole by a magnet-type snapping mechanism.

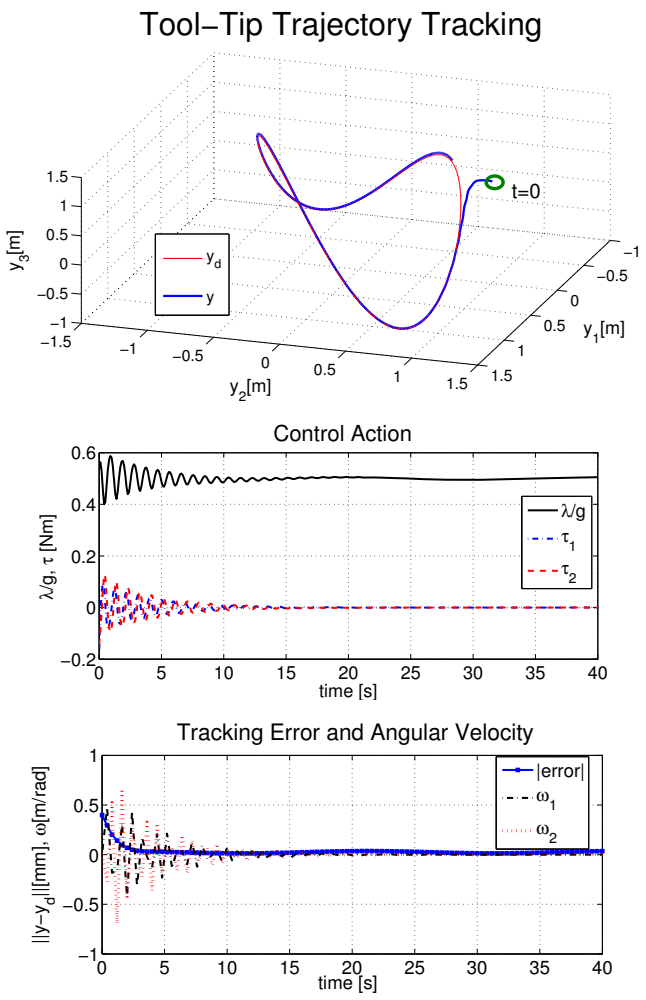

Figure 5. Tool-tip position y trajectory tracking control: 1) trajectory of y_d and y; 2) control action λ, τ; 3) tracking error $e := y - y_d$ and angular rate w.

Now, suppose that we want to rotate the tool along the N^B-axis while keeping $N^B = N^o$ and $y \approx 0\ \forall t \geq 0$ from $R(0) = I$ (e.g., **screwdriver operation**). For this case, the rotation matrix R of the quadrotor can be written as (10) with $w = [w_1; 0; 0]$ and $w_1 = \dot{\theta}_1$, and, similar to (11), we can obtain

$$-R^T f_e = \begin{pmatrix} 0 \\ -md_3\dot{w}_1 + mg\sin\theta_1 \\ -md_3 w_1^2 - \lambda + mg\cos\theta_1 \end{pmatrix} \qquad (17)$$

where $-R^T f_e$ represents the contact force represented in the body-frame $\{B\}$.

This relation (17) then shows that the tool rotation motion itself will not generate any force along the direction of N^B (=N^o), which, yet, is usually necessary to maintain the quadrotor-environment contact. Due to this reason, in practice, we would

need some external means to maintain this contact even in the presence of, e.g., parametric uncertainty, noise, actuator calibration error, etc. Some of such means between the work site and the tool-tip include: magnetic snapping mechanism as stated above; flexible compliance coupling; or a combination of these two. For the simulations below, we incorporate this contact-maintaining force by a simple damper-spring interaction-force model, i.e., $f_e := -B\dot{y} - Ky$.

Even with such contact-maintaining mechanisms in place, we would still need to regulate $-R^T f_e$ to be possible so that the perturbing force do not overpower those mechanisms. From (17), we can then see that $-R^T f_e = 0$ can be achieved if we drive $\theta_1, w_1, \dot{w}_1$ to satisfy the dynamics of (17) with $f_e = 0$. For this, note that, if $d_3 < 0$, the dynamics in the second row is again similar to the stable dynamics of downward pendulum. This suggests us to choose the desired angle $\theta_1^d(t)$ for θ_1 to be

$$\theta_1^d(t) := \theta_{\max} \sin w_n t \tag{18}$$

with $w_n := \sqrt{\frac{g}{|d_3|}}$, which is the solution of the linearized dynamics in the second row of (17) about $\theta_1(0) = 0$; and to choose the thrust command λ s.t., from the third-row of (17),

$$\lambda = mg\cos\theta_1 - md_3 w_1^2$$

with the attitude torque command also given similar to (15)

$$\tau = w \times Jw + J[\dot{w}_d - \alpha(w - w_d) - \beta(\theta - \theta_d)] - \tau_c \tag{19}$$

where $w_d = [\dot{\theta}_1^d; 0; 0]$, $\theta_d = [\theta_1^d; 0; 0]$, $\theta = [\theta_1; 0; 0]$, with which the attitude dynamics (2) is reduced to a linear second-order stable dynamics of $(\theta_1 - \theta_1^d) \in \Re$ (instead of that in SO(3)), since here we confine the rotation motion only along the N^B-axis. Note also that, since the attitude dynamics is passive and fully-actuated [18], there are many ways to reduce (or reject) the effect of even uncertain τ_c as long as τ is powerful enough than τ_c (e.g., high-gain feedback; sliding mode control).

Simulation results with this tool rotating control law are given in Fig. 6, where we can see that: 1) the quadrotor's center-of-mass position x makes a circular trajectory, suggesting the tool rotation; 2) both f_e and y is small, yet, not perfectly zero, since we inject some parametric uncertainty while computing the control action (λ, τ) and also the desired trajectory θ_1^d (18) is a solution of the linearized dynamics, not the original nonlinear dynamics; and 3) control actions $(\lambda, \tau_1, \tau_2)$ are a bit aggressive. To reduce this control aggressiveness, we slow down the desired oscillation frequency to be $w_n/2$, and the results are also presented in Fig. 6, where we can see that control action is now smoother than those with $w = w_n$. However, f_e and y now become bigger than those with $w = w_n$ in Fig. 6, since θ_1^d is not the solution of the second-row dynamics of (17) anymore, thus, deploying this

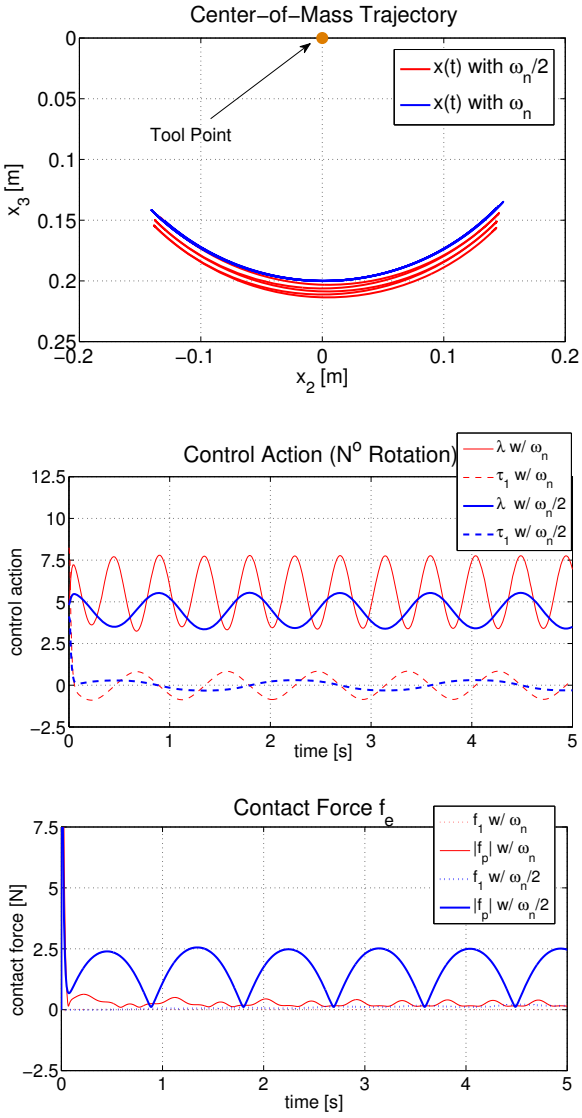

Figure 6. Tool rotation control about the N^o-axis with $\theta_1^d = \theta_{\max} \sin w_n t$: 1) trajectory of center-of-mass x (note that positive x_3 implies downward direction); 2) control action λ, τ; 3) contact force f_e (with $f_1 = f_{e1}, f_p = \sqrt{f_{e2}^2 + f_{e3}^2}$).

θ_1^d produces a larger perturbation to the y-dynamics, to the contact force $|f_e|$ and, consequently, to the circular trajectory of the x-position as well. How to design the motion command for θ_1^d other than (18), which can further reduce the effect of f_e while still achieving the tool operation motion is a topic for future research.

Let us also consider the tool rotation operation about the axis of $E^o = E^B$, with the quadrotor's x-position translational motion being confined within the (N^o, D^o)-plane (e.g., **vertical jack** op-

eration). Then, similar to above, using (12), we can obtain

$$-R^T f_e = \begin{pmatrix} md_3\dot{w}_2 - md_1 w_2^2 - mg\sin\theta_2 \\ 0 \\ -md_1\dot{w}_2 - md_3 w_2^2 - \lambda + mg\cos\theta_2 \end{pmatrix} \qquad (20)$$

where $w_2 = \dot{\theta}_2$. We then also aim to regulate this $-R^T f^e$ to be possible to avoid a separation between the tool-tip and the work-site. Here, in contrast to (17), the first-row dynamics is not the dynamics of the pendulum anymore. However, its linearized dynamics is locally-stable and still assumes the expression of

$$\theta_2^d(t) = \theta_{\max}\sin w_n t, \quad w_n = \sqrt{g/|d_3|}$$

similar to above. We choose this $\theta_2^d(t)$ as the desired trajectory for $\theta(t)$ and design the attitude torque input τ similar to (19). We also design the thrust control input λ s.t.

$$\lambda = -md_1\dot{w}_2^d - md_3 w_2^2 + mg\cos\theta_2$$

where $\dot{w}_2^d = \ddot{\theta}_2^d(t)$.

We perform simulation for this tool rotation control about the E^o-axis and present the results in Fig. 7, where we use $w = w_n/2$ instead of $w = w_n$, since this latter case turns out to require aggressive control action (e.g., $\lambda < 0$ at some points). From Fig. 7, we can then see that, since we use more approximation here than for the case of $w = w_n$ in Fig. 6, a larger perturbation to the tool-tip position y and to the contact force f_e are evident, while the control action λ, τ are smoother here. How to planning $\theta_2^d(t)$ to further reduce f_e while still achieving the tool rotation task is a topic for future research. Experimental implementation to validate the proposed control laws in the presence of parametric uncertainty, un-modeled dynamics, imperfect control actuation, aero-dynamics disturbance, etc., with the tool-worksite coupling as mentioned above, is under way and will be reported in a future publication.

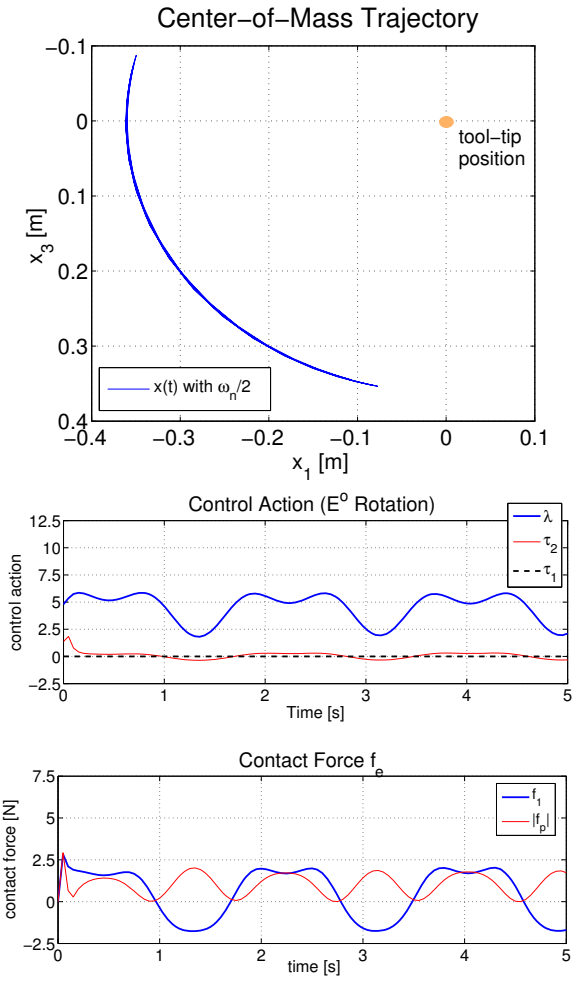

Figure 7. Tool rotation control about the N^o-axis with $\theta_1^d = \theta_{\max}\sin w_n t$: 1) trajectory of center-of-mass x (note that positive x_3 implies downward direction); 2) control action λ, τ; 3) contact force f_e (with $f_1 = f_{e1}, f_p = \sqrt{f_{e2}^2 + f_{e3}^2}$).

5 Conclusion

In this paper, we propose novel control frameworks for a quadrotor to control a mechanical tool (e.g., screwdriver, wrench, vertical jack), which is rigidly-attached on the quadrotor and whose control requires an *integrated and simultaneous* control of the quadrotor's translation and rotation. In particular, we address the two basic behaviors for the quadrotor tool-operation: 1) tool-tip position trajectory tracking; and 2) tool rotation control while regulating the tool-tip position. We elucidate a certain structural condition for generating arbitrary control action to control the tool-tip position while avoiding internal dynamics instability (with possible finite-time escape). Simulation is also performed to support/illistrate the theory.

Some possible future research directions include: 1) extension of the proposed control frameworks for other type of quadrotor tool operation; 2) robust prevention of the finite-time escape even if $d_3 > 0$; and 3) experimental implementation and verification using real quadrotors.

ACKNOWLEDGMENT

Research supported in part by the Basic Research Laboratory program of the National Research Foundation of Korea (NRF) grant funded by the Korea government (MEST) (No. 2009-0087640); and the Engineering Research Institute and Research Settlement Funds at Seoul National University.

REFERENCES

[1] Kumar, V., and Michael, N., 2011. "Opportunities and challenges with autonomous micro aerial vehicles". In Proc. of Int'l Symposium on Robotics Research.

[2] Vachtsevanos, G., and Valavanis, K., eds., 2006. *IEEE Robotics and Automation Magazine: Special Issue on Unmanned Aerial Vehicles*, Vol. 13. September.

[3] Frazzoli, E., Dahleh, M. A., and Feron, E., 2000. "Trajectory tracking control design for autonomous helicopters using a backstepping algorithm". In Proc. American Control Conference, pp. 4102–4107.

[4] Mahony, R., and Hamel, T., 2004. "Robust trajectory tracking for a scale model autonomous helicopter". *International Journal of Robust and Nonlinear Control,* **14**, pp. 1035–1059.

[5] Hua, M.-D., Hamel, T., Morin, P., and Samson, C., 2009. "A control approach for thrust-propelled underactuated vehicles and its application to vtol drones". *IEEE Transactions on Automatic Control,* **54**(8), pp. 1837–1853.

[6] Roberts, A., and Tayebi, A., 2011. "Adaptive position tracking of vtol uavs". *IEEE Transactions on Robotics,* **27**(1), pp. 129–142.

[7] Lee, D. J., Ha, C., and Zuo, Z., 2012. "Backstepping control of quadrotor-type uavs: trajectory tracking and teleoperation over the internet". In Proc. Int'l Conf. on Autonomous Systems. To appear.

[8] Purwin, O., and D'Andrea, R., 2009. "Performing aggressive maneuvers using iterative learning control". In Proc. IEEE Int'l Conference on Robotics & Automation, pp. 1731–1736.

[9] Mellinger, D., Michael, N., and Kumar, V., 2010. "Trajectory generation and control for precise aggressive maneuvers with quadrotors". In Proc. of Int'l Symposium on Experimental Robotics.

[10] Stramigioli, S., Mahony, R., and Corke, P., 2010. "A novel approach to haptic tele-operation of aerial robot vehicles". In Proc. IEEE Int'l Conf. on Robotics & Automation, pp. 5302–5308.

[11] Lee, D. J., Franchi, A., Giordano, P. R., Son, H.-I., and Bülthoff, H. H., 2011. "Haptic teleoperation of multiple unmanned aerial vehicles over the internet". In Proc. IEEE Int'l Conference on Robotics & Automation, pp. 1341–1347.

[12] Abdessameud, A., and Tayebi, A., 2009. "Formation control of vtol-uavs". In Proc. IEEE Conference on Decision & Control, pp. 3454–3459.

[13] Lee, D. J., 2011. "Distributed backstepping control of multiple thrust-propelled vehicles on balanced graph". In Proc. IFAC World Congress.

[14] Lee, D. J., 2012. "Distributed backstepping control of multiple thrust-propelled vehicles on balanced graph". *Automatica*. Conditionally accepted.

[15] Michael, N., Fink, J., and Kumar, V., 2011. "Cooperative manipulation and transportation with aerial robots". *Autonomous Robots,* **30**, pp. 73–86.

[16] Mellinger, D., Shomin, M., Michael, N., and Kumar, V., 2010. "Cooperative grasping and transport using multiple quadrotors". In Proc. Intl. Symposium on Distributed Autonomous Robotic Systems.

[17] Khalil, H. K., 1995. *Nonlinear systems*, second ed. Prentice-Hall, Upper Saddle River, NJ.

[18] Sepulchre, R., Jankovic, M., and Kokotovic, P., 1997. *Constructive nonlinear control*. Springer-Verlag, London.